

International Symposium on Structural Intermetallics
Seven Springs Resort, Pennsylvania
September 1997
(accepted April 1997; to appear in the proceedings)

EQUILIBRIUM POINT DEFECTS IN NiAl AND SIMILAR B2
 INTERMETALLICS STUDIED BY PAC

Gary S. Collins* , Jiawen Fan[†] and Bin Bai

Department of Physics
 Washington State University
 Pullman, WA 99164-2814, USA

Abstract

Point defects in NiAl and other structural intermetallics have been studied using perturbed angular correlation of gamma rays (PAC), by which signals are detected from antisite atoms and/or lattice vacancies in the first few atomic shells of probe atoms. For samples of quenched NiAl having 50 to 54 at.% Ni, site-fractions of Ni-vacancies (proportional to the vacancy concentration) were found to be independent of composition, indicating that the equilibrium, high-temperature defect is the Schottky vacancy pair and not the so-called triple defect. An effective formation enthalpy of 1.11(4) eV was measured for Ni-vacancies after equilibrating and quenching samples from temperatures in the range 700-1400 C. The formation enthalpy of the Schottky pair is two times larger. Quenched-in vacancies exhibit striking, novel behavior at low temperature: vacancies start to become mobile at about 350 C in 15-minute anneals, as observed by trapping at the probe atoms, but are only able to anneal out appreciably at temperatures of about 700 C. This behavior is attributed to different mobilities of Ni and Al vacancies. Recent data suggests that the Al-vacancy becomes thermally activated at about 350 C, converting into a Ni-vacancy and Ni-antisite atom when it comes near the probe atom. The Ni-vacancy becomes mobile only at about 700 C. Thermal activation of motion of quenched-in and confined vacancies at low temperature, observed here for the first time, offers an explanation for the well-known transition from brittle-to-ductile mechanical behavior in NiAl near 300 C. The explanation is supported by a study of vacancy interactions with Zr solutes that is briefly described. Results for other B2 intermetallics are also briefly described.

* *Corresponding author, email: collins@wsu.edu;*
research group URL: <http://defects.physics.wsu.edu/>

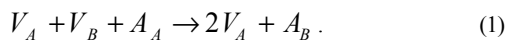
[†] *Now with North American Scientific, North Hollywood, CA.*

Introduction

There is considerable interest in developing highly-ordered intermetallic compounds such as NiAl as high-temperature structural materials. Properties of these materials are affected by intrinsic point defects such as antisite atoms and lattice vacancies. Because vacancies mediate diffusion and diffusion-related processes such as creep, it is particularly important to understand their properties. The present paper describes experiments carried out toward that end.

NiAl and other compounds such as CoAl and PdIn that have the CsCl (B2) structure and are formed from group VIIIA and IIIB are well-ordered up to their melting temperatures. We shall use the notation AB to generically identify these compounds, with A= Ni, Co, Pd, and B= Al, In, et cetera. They exist as single phases for compositions typically extending to several atomic percent on either side of stoichiometry. Deviations from stoichiometry are accommodated by introduction of structural point defects. Density and lattice parameter measurements on annealed samples have shown (1) that compounds deficient in element A (A-poor) normally contain vacancies on the A-sublattice (V_A) whereas A-rich compounds contain A atoms as antisite defects on the B-sublattice (A_B). (Symbols identify the type of atom or defect and subscripts indicate the sublattice on which it sits.) For a review of this data, see Chang and Neumann (2). It should be noted that the concentrations of structural defects needed to accommodate deviations from stoichiometry can be very large: annealed NiAl having 49 or 51 at.% Ni will have mole fractions equal to 4 at.% for V_{Ni} or 2 at.% for Ni_{Al} , respectively. (Mole fractions are defined in this paper with respect to the total number of sites on a single sublattice.)

Equilibrium point defects become thermally activated at elevated temperature to minimize the free energy of the crystal. Considering single-phase systems like B2 NiAl, equilibrium defects can only be created as combinations of elementary defects that maintain strictly equal numbers of lattice sites on all sublattices. Possible defects include the Schottky defect and so-called triple defect. Excluding interstitial defects because of their high energy, the available elementary defects are vacancies and antisite atoms on the two sublattices. Of these, B_A (e.g., Al_{Ni}) will be excluded from consideration because it is unobserved as a structural defect in A-poor alloys and therefore must have high energy. From the three remaining elementary defects V_A , V_B and A_B can be formed two defect combinations: the Schottky vacancy-pair, $V_A + V_B$, and the triple-defect originally proposed by Wasilewski (3), $2V_A + A_B$. The triple defect can be imagined to form from a Schottky defect by transfer of an A_A atom to a neighboring B-vacancy, thereby creating a second A-vacancy and A-antisite atom:



The Schottky and triple defects are homogeneous defects in the sense that they can be generated without changing the local atomic composition. The principal defect activated will be the one having the lower formation enthalpy. In the following we shall assume that electron-screening leads to small interaction energies between the elementary defects, as borne out by calculations (e.g., ref. 5). However, little is known experimentally on this point.

Other mechanisms for forming defects must also be considered. A possible mechanism is preferential evaporation of a constituent, modifying the composition. A second mechanism is formation of low-dimensional phases at surfaces, grain boundaries or dislocations. A simple example of the latter mechanism would be termination of a NiAl lattice with Ni-sites at surfaces and grain-boundaries. In effect, this would make for a greater number of sites on the Ni sublattice. As a consequence, the Ni composition within the grains would be reduced. In our experiments, described below, the typical grain size was about 150 microns (4), for which there is a ratio of 10^{-5} surface to volume sites. Thus, even complete enrichment of the surface with Ni would modify the composition within the grains by a small, undetectable amount. Formation of enriched multilayers amounts to phase separation, and so is ruled out for these B2 systems by the phase diagrams. We therefore expect that presence of heterogeneous defects will only lead to small and unimportant shifts in the elemental composition within grains. For our grain size, enrichment of a Ni monolayer could cause formation of a mole fraction of 10^{-5} Ni-vacancies. Vacancy defect concentrations in quenched NiAl are much greater, of the order of 10^{-3} , so that mole fractions of heterogeneous elementary defects such as might be produced by surface enrichment are expected to be small in comparison to concentrations of homogeneous Schottky or triple defects.

Equilibrium concentrations of defects become established by diffusion. Atom movement in NiAl and similar compounds almost certainly occurs by vacancy diffusion. A recent calculation for stoichiometric NiAl indicates that the dominant diffusion mechanism involves Ni and Al vacancies making near-neighbor jumps on their own sublattices (that is, second-neighbor jumps on the underlying bcc lattice), (5) and we will assume this is true for slightly Ni-rich compositions (50-53.5

at.% Ni) considered below. As a consequence, in order to form either Schottky or triple-defects during heating, vacancies on both sublattices must diffuse in from the surface. As long as equal numbers of both vacancies diffuse in, the composition remains homogeneous. Once inside, an Al-vacancy may react with a host Ni atom to form, in effect, a triple-defect (cf. eq. 1):



Since there is no other obvious way for triple-defects to form, diffusion of V_{Al} appears to be essential even if the triple-defect were the dominant equilibrium defect. Interestingly, recent calculations of defect energies in NiAl (5,6) indicate that the triple-defect has a formation energy lower than the Schottky defect, but that Al-vacancies have a migration energy lower than Ni-vacancies. Thus, equilibrium could be established under the triple-defect model as follows: V_{Al} diffuse rapidly from the surface and convert into V_{Ni} and an immobile Ni_{Al} (eq. 2 above). Later, either the same V_{Ni} or other V_{Ni} migrating nearby may undergo the reverse reaction with the immobile Ni_{Al} , recreating the more mobile V_{Al} . Such serial conversion between mobile and immobile states is akin to the problem of hydrogen diffusion in a medium with shallow traps. Therefore, V_{Al} may contribute significantly to diffusion even when its instantaneous concentration is low. To summarize, diffusion of both types of vacancies is necessary under either model.

What is known about the equilibrium defect in NiAl? Considering NiAl, Wasilewski used qualitative arguments to show that the triple-defect might be the dominant equilibrium defect in compounds like NiAl(3). However, from the extensive review of properties of NiAl by Miracle (7), identification of the equilibrium defect to date appears inconclusive. This is because experimental methods used have been indirect. Recent computations of defect structures and energies in NiAl (e.g. refs. 5,6,8) find that the Schottky defect has a higher formation enthalpy than the triple-defect.

In the present work, we apply a microscopic method, perturbed angular correlation of gamma rays (PAC), to study equilibrium defects in NiAl directly. With this method, we are able to observe signals due to elementary defects near probe atoms sitting on the Al-sublattice. These signals have been identified with V_{Ni} in the first atomic shell and Ni_{Al} or V_{Al} in shell 2, and with combinations of those defects. Following a description of the method, we describe four experiments on NiAl with goals and results as follows:

(1) Nature of the equilibrium defect. Five samples with compositions spanning the range 50.3-53.5 at.% Ni were quenched rapidly after equilibration at a fixed temperature of 1050 C. The site-fraction of probe atoms having a V_{Ni} neighbor (proportional to the Ni-vacancy concentration) was found to be independent of composition. This result is shown to be consistent with the Schottky-defect model and not the triple-defect model.

(2) Formation enthalpy of the equilibrium defect. Two samples having 50.7 at.% Ni were equilibrated and quenched from high temperatures. Site-fractions of V_{Ni} increase with quenching temperature in the range 700-1400 C, with an effective activation enthalpy equal to 1.11(4) eV. This effective formation enthalpy for V_{Ni} translates to an activation enthalpy for a Schottky pair equal to 2.22(8) eV.

(3) Low-temperature equilibrium regime for quenched-in defects. Annealing out of excess defects was studied in samples having 50.6 at.% Ni. Vacancy mobility was first observed at 350 C in 15 min. isochronal anneals by formation of increasing numbers of V_{Ni} defects next to the probe atoms. Additional studies showed, unexpectedly, that over the range of 350-650 C vacancies are unable to anneal out to any appreciable extent. Further measurements elucidated for the first time a novel low-temperature equilibrium regime in which a concentration of mobile vacancies is confined in the lattice. A possible explanation for this phenomenon is that one of the two vacancy species migrates at 350 C while the other migrates at 650 C. In the intervening temperature range, one of the two species is mobile with a constant concentration. The mobile vacancy species may therefore contribute in novel ways to diffusion processes at low temperature. Existence of this regime offers a possible explanation for the onset of ductile mechanical behavior at about 300 C.

(4) Identity of the vacancy species diffusing at 300 C. Annealing quenched samples at 350 C leads to an increase in the site-fraction of V_{Ni} complexes, and was initially therefore naturally attributed to migration and trapping of V_{Ni} . (9) However, recent measurements show that, when trapping starts, there is a significant increase in the site fraction of a new signal attributed to a complex of V_{Ni} and V_{Al} defects near the probe. This and other data can be explained by migration of V_{Al} to a position close to a probe atom (in shell 2, 3 or 5, belonging to the Al-sublattice) followed by conversion into a first-shell V_{Ni} defect and immobile Ni_{Al} antisite atom in shell 2, 3 or 5 (see eq. 2). Therefore, the more mobile vacancy is identified as V_{Al} .

Methods

Sample preparation.

NiAl samples of about 100 mg total mass were made by arc-melting ~5N pure foils of Ni and Al together with radioactive ^{111}In under argon. Nominal compositions were taken to be the actual ones since mass losses during arc-melting were very small and lead only to uncertainties in the composition of about 0.1 at.%. After melting, samples were annealed for 1 hour under hydrogen at 1200 C in a tube furnace in order to coarsen the grains and improve sample homogeneity. Based on inhomogeneous broadening of PAC signals caused by distant defects in a series of alloys from 48-52 at.% Ni, (9) compositional uniformity across the samples is believed to have been better than 0.2 at.%.

Samples were quenched rapidly from temperatures up to 1400 C using a vertical drop-furnace (10) having a quenching rate estimated to be approximately 10^4 K/s.

Perturbed angular correlation of gamma rays (PAC).

General approach. Defects are detected via the radiations emitted by radioactive probe atoms introduced for this purpose in the host. For the $^{111}In/Cd$ probe used in this study, mole fractions of probes are typically about 10^{-8} , excluding any appreciable disturbance of defect behavior by probes. A crystal defect produces an electric-field gradient (efg) in its vicinity

that falls off with distance r qualitatively as r^{-3} . The most significant and best-resolved efg's will therefore be produced by defects in neighborhoods of a few atomic shells around the PAC probes. A defect's efg interacts with the quadrupole moment of the nuclear PAC level, which has spin-5/2 and a half-life of 84 ns. This so-called hyperfine interaction can be considered to cause the probe's nuclear spin to precess over lifetime with a frequency characteristic of the defect type and its distance from the probe (atomic shell). The interaction is detected through the time and angular correlation of gamma radiations emitted when the PAC level is formed and decays. One measures a lifetime decay curve for the PAC level that is modulated by a perturbation function $G_2(t)$. The perturbation function contains all the information about the defects. Further information on methods may be found in ref. (11).

For a unique efg, the perturbation function of a spin-5/2 PAC level is given by

$$G_2(t) = s_0 + s_1 \cos \omega_1 t + s_2 \cos \omega_2 t + \cos \omega_3 t, \quad (3)$$

in which the three frequency harmonics are related via $\omega_3 = \omega_2 + \omega_1$ and $1 \leq \omega_2 / \omega_1 \leq 2$, and the amplitudes s_0 - s_3 sum to unity. The fundamental frequency ω_1 is proportional to the principal component of the efg tensor, V_{zz} , and the ratio ω_2 / ω_1 is related to the asymmetry parameter of the efg tensor, $\eta = (V_{xx} - V_{yy}) / V_{zz}$. When there is a three-fold or higher axis of charge symmetry through the probe nucleus, the interaction is said to be axially symmetric ($\eta = 0$), $\omega_1 : \omega_2 : \omega_3$ are in the proportion 1:2:3, and the amplitudes s_0 - s_3 are 1/5, 13/35, 10/35 and 5/35, respectively. In that case, $\omega_1 = \frac{3\pi}{10} \frac{eQV_{zz}}{h}$, in which Q is the quadrupole moment of the nucleus. For lower symmetry, $0 < \eta < 1$. Finally $\omega_1 = 0$ if the point symmetry is cubic as in the perfect B2 crystal.

In a typical measurement there is a variety of local environments of probes due to the presence of structural and/or thermal defects. Each environment produces a characteristic value of ω_1 and η . In practice one observes a superposition of perturbation functions for all environments, each multiplied by an amplitude proportional (in a known way) to the fraction f of probes in that site. The hyperfine parameters ω_1 and η and site fractions f are obtained by fitting experimental spectra by computer to a sum of $G_2(t)$ functions.

PAC spectrometer. We used a four-detector spectrometer of standard design with BaF_2 scintillators. A more detailed description of instrumentation is given in ref. (11).

Defect identification

Identifying signals with underlying geometrical arrangements of atoms was mostly made through measurements on annealed samples having 48-52 at.% Ni. (12,9) The ^{111}In probes are almost certainly located on the Al sublattice because In is isovalent with Al and has a large atomic size like Al. Since the Al_{Ni} antisite is an unobserved high-energy defect, an even larger In_{Ni} impurity is *a fortiori* less likely. In table I are given atom types and distances of atoms from shells near In_{Al} probes

in perfect, stoichiometric NiAl. Distances are in units of the near-neighbor distance r_{nn} . Also listed are inverse-cubed distances to indicate the relative strengths of efg's that might be expected from defects in different shells.

Table I. Atom shells near In_{Al} probes in perfect NiAl.

Shell	Atom	Number	r/r_{nn}	$(r_{nn}/r)^3$
1	Ni	8	1.0000	1.000
2	Al	6	1.1547	0.650
3	Al	12	1.6330	0.230
4	Ni	24	1.9149	0.142
5	Al	8	2.0000	0.125

The experimental efg of a defect may be taken to be proportional to the product of r^{-3} in the table and a (shell-dependent) effective charge. Table I shows that stronger efg's are likely to come preferentially from defects in the first and second shells. Indeed, we believe this is the case in our measurements. More distant defects produce weaker efg's that lead only to inhomogeneous broadening of signals due to nearby defects.

Local configurations anticipated for defects are shown by diagrams in Figure 1. Attention is restricted to defects in the two closest shells. Lines in the diagrams show the Ni-sublattice, with Ni sites are at cube corners and Al sites at cube centers (Ni and Al atoms on their normal sites are not drawn.) Symbols indicate In_{Al} probes (large shaded circles), V_{Ni} in the first atomic shell (open squares), and Ni_{Al} (small shaded circles) and V_{Al} (stippled square) in the second atomic shell. Thick lines are drawn between probes and defects to make the geometries of the defect-probe complexes clearer.

Experimental hyperfine interactions measured at 295 K are listed in Table II together with identifications of sites in terms of local environments of the probes. A relative measure of interaction strength is indicated by the ratio of ω_1 to the monovacancy frequency. The V_{Al} configuration was not observed by itself, but the analogous V_{In} site that has been unambiguously identified in PdIn (13,14) has a very low frequency, so that a correspondingly low frequency is expected in NiAl. Diagrams from Fig. 1 are also listed.

Table II. Quadrupole interactions and environments of probes

ω_1 (Mrad/s)	η	$\omega_1 / \omega_1^{\text{V}}$	Local Environment ^a	Figure
~ 0	-	~ 0	defect-free In_{Al}	1.a
128(1)	0	(1)	V_{Ni}	1.b
187(1)	0.64(1)	1.46(1)	2 V_{Ni} (a)	1.c
222(2)	0.89(1)	1.73(1)	2 V_{Ni} (b)	1.d
19(2)	0.1(1)	0.15(2)	Ni_{Al}	1.e
unobserved	-	(0.15) ^b	V_{Al}	1.f
141(2)	0.20(5)	1.10(2)	$\text{V}_{\text{Ni}} + \text{Ni}_{\text{Al}}$	1.g&h
158(2)	0.20(5)	1.23(2)	$\text{V}_{\text{Ni}} + \text{V}_{\text{Al}}$	1.j&k

a. V_{Ni} are in shell 1 and Ni_{Al} and V_{Al} are in shell 2.

b. Ratio measured in PdIn, refs. (13,14).

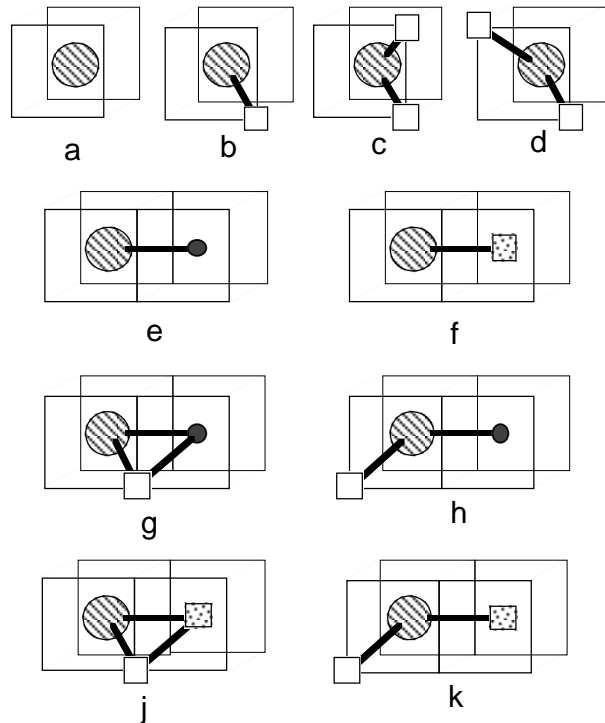


Figure 1: Possible configurations of In probe atoms and nearby point defects. Symbols: In-probe (large shaded circle); Ni-vacancy (open square); Al-vacancy (stippled square); Ni-antisite atom (small black circle). The cubic grid represents the Ni sublattice. Host atoms on normal sites are not drawn.

Most configurations were first observed in measurements made on a series of five NiAl alloys with compositions in the range 48-52 at.% Ni. PAC spectra measured after annealing at 1200 C and cooling in furnace to room temperature over about 12 hours are shown in Figure 2.(9,11,12)

Knowledge of structural defects in Ni-poor and Ni-rich samples, V_{Ni} and Ni_{Al} respectively,(1) helps identify signals with sites. The arguments for identification are given briefly here. More information can be found in refs. (9,11,12).

Defect-free and V_{Ni} sites. The 50.1% sample exhibits a zero-frequency signal (raised baseline) for about 50% of the probe atoms that is consistent with cubic point symmetry and is attributed to defect-free, stoichiometric NiAl (Fig. 1.a). The perturbation with period ~ 50 ns has axial symmetry and is attributed to one V_{Ni} in the first atomic shell (Fig. 1.b). The interaction frequency, 128 Mrad/s, is comparable to frequencies observed for near-neighbor vacancies trapped to ^{111}In probes in pure metals.(15) (The large site fraction of V_{Ni} is not obviously expected for this composition, it is attributed to incomplete annealing out of vacancies during furnace-cooling and/or to the presence of structural vacancies in parts of the sample caused by chemical inhomogeneity that made portions of the sample slightly Ni-poor.)

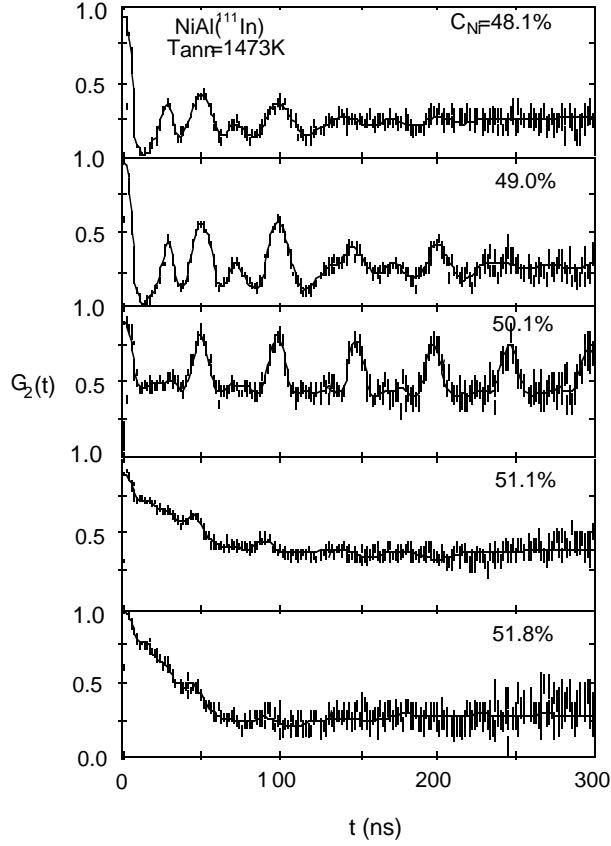


Figure 2: PAC spectra of annealed NiAl (48.1-51.8 at.% Ni). From ref. 11.

Double V_{Ni} sites. Ni-poor spectra (48.1 and 49.0%) exhibit a large site fractions of the 128 Mrad/s signal and, as well, the higher frequency 187 and 222 Mrad/s signals. The expected mole fractions of structural V_{Ni} are 7.6% and 4.0%, respectively. The high frequency signals are attributed to two distinct configurations of two V_{Ni} in the first shell (Figs. 1.c and 1.d). The V_{Ni} defects bind with In_{Al} probes. Evidence for binding comes from the fact that site fractions of the V_{Ni} in both Ni-poor spectra are greater than what would be expected if the structural vacancies were at random. At a value of 45%, the site-fraction of the 128 Mrad/s signal exceeds the maximum possible probability for having a single defect neighbor assuming that defects are located at random, confirming nonrandomness.

Ni_{Al} site. Ni-rich spectra (51.1 and 51.8%) exhibit mostly low-frequency interactions that were originally attributed to distant defects (11,12). However, among these is a unique 19 Mrad/s signal that was attributed more recently (9) to one Ni_{Al} in the second shell (Fig. 1.e). The site fraction of the unique 19 Mrad/s signal is always much greater than expected on the basis of a random distribution of antisite atoms. This will be discussed further below.

Mixed V_{Ni} and Ni_{Al} sites. Ni-rich spectra in Fig. 2 have small site fractions of a signal with 141 Mrad/s and small efg

asymmetry parameter. Since the only high-frequency structural defect is the first-shell V_{Ni} , it is assumed to involve a quenched-in V_{Ni} and a second shell Ni_{Al} structural defect in configurations Fig. 1.g or 1.h. Both configurations lead to the same efg calculated in the point-charge approximation, and are therefore equivalent in our measurements. The point-charge calculations show that one can explain the 128, 19 and 141 Mrad/s signals reasonably well using an effective charge of the Ni_{Al} defect equal to -0.4 of the charge of V_{Ni} . (9)

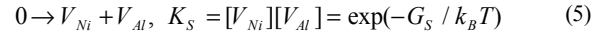
Signal identifications from the past work described above are believed to be fairly robust. The remaining signal in Table II, with 158 Mrad/s, was observed for the first time only recently. Its tentative identification as a first-shell V_{Ni} and second-shell V_{Al} complex is discussed separately below under experiment 4. Among the simple configurations shown in Fig. 1, only the single V_{Al} complex has not been observed.

Thermodynamics of Defects

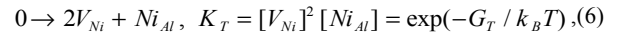
Thermodynamic properties of the point defects can be related to the observed site fraction of V_{Ni} using the law of mass action. Further details will be found in ref. (9). We write for the composition $Ni_{1+2x}Al_{1-2x}$, in which x marks the deviation from stoichiometry. Defining mole fractions of the defects with respect to the number of sites on one sublattice, and assuming $[Al_{Ni}]=0$, it is easy to show that mole fractions of defects obey the following equation of constraint:

$$4x + (1 - 2x)[V_{Ni}] - (1 + 2x)[V_{Al}] = 2[Ni_{Al}]. \quad (4)$$

The reaction for formation of a Schottky defect and its equilibrium constant are



and similarly for the triple-defect,



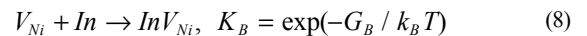
in which 0 specifies the defect-free lattice. Substituting $[V_{Al}]$ from eq. 5 and $[Ni_{Al}]$ from eq. 6 into eq. 4 leads to a general, cubic equation in $[V_{Ni}]$.

Measurements were made on slightly Ni-rich samples. Under the Schottky defect model, only structural Ni_{Al} are present, so that $[Ni_{Al}] = 2x$, and one obtains for small positive x:

$$[V_{Ni}] = [V_{Al}] = \exp(S_S / 2k_B) \exp(-E_S / 2k_B T). \quad (7)$$

Thus vacancy mole-fractions on the two sublattices are equal and, moreover, independent of composition. Under the triple-defect model, on the other hand, $[V_{Ni}]$ depends significantly on x for small x. Therefore, measurement of the x-dependence of $[V_{Ni}]$ can be used to distinguish between the two defect models, as we do in experiment 1 below.

Ni-vacancies tend to bind with In probes, as already demonstrated by enhanced site fractions in Fig. 2. This can be modeled by a reaction for forming a vacancy-probe complex:



where G_B is the free energy of binding of the first vacancy. Similar reactions can be written down for binding of additional vacancies (with different binding enthalpies). Defining the site fractions for probes that have n near-neighbor vacancies as f_n , it can be shown (9) that the monovacancy site-fraction has a remarkably simple relation to thermodynamic quantities after it has been normalized by the defect-free fraction, $f_0 = 1 - f_1 - f_2 - \dots$:

$$\frac{f_1}{1 - f_1 - f_2} = zK_B[V_{Ni}], \quad (9)$$

in which z is the coordination number (8 here). Nontrivially, Equation 9 is independent of the defect model or of binding of additional vacancies to the probe atom; f_1/f_0 is simply proportional to the product of the vacancy concentration and the equilibrium constant for binding of the first vacancy.

Experiments and results

Experiments reported below were made on samples with 50.3-53.5 at.% Ni. Thus, the only expected structural defects are Ni_{Al} antisite atoms.

1. Identity of the equilibrium defect in NiAl

Five samples of NiAl were each equilibrated at 1050 C and then rapidly quenched to room temperature. (9) Special care was taken to ensure that all samples received the same thermal treatment. In Figure 3 is shown the normalized monovacancy site fractions versus x , the deviation from stoichiometry. In the next paragraph it is explained that K_B in equation 9 depends only on the quenching rate. Since quenching rates were the same for all samples, then, from equation 9, site fractions should be proportional to the vacancy concentration. The figure shows that quenched-in site fractions are independent of composition. Drawn over the figure are curves showing expected trends for the Schottky and triple-defect models. (The triple-defect curve was calculated assuming a vacancy mole fraction of about 10^{-3} .) As can be seen, the lack of dependence of the quenched-in site fraction on composition is in excellent agreement with the Schottky model and, at least for our samples, appears to rule out the triple-defect model. Additional measurements in ref. 9 (not shown) obtained after quenching from in the range 800-1000 C exhibit the same lack of dependence on composition. Alternative explanations for this independence include possibilities that (1) defects might form by an unknown, heterogeneous mechanism in our samples, or (2) there might exist a significant dependence of the defect formation or vacancy migration enthalpies on x that compensates by accident for the dependence based on the defect model.

2. Formation enthalpy of the equilibrium defect

PAC measurements were made on 50.6 at.% Ni samples after rapid quenching from temperatures in the range 200-1400 C. (9) Some spectra from in the high-temperature range 700-1400 C are shown in Figure 4. Samples were equilibrated for 1 hour and were determined by comparison with spectra measured after different equilibration times to be in equilibrium prior to quenching. The summed site-fraction of first-shell single-

vacancy defects (128 and 141 Mrad/s) increases rapidly with temperature. The normalized monovacancy site fraction is plotted versus inverse temperature in Figure 5. As can be seen, the site fraction has a well-defined Arrhenius behavior above about 750 C with activation enthalpy 1.11(4) eV. To interpret the activation enthalpy, it was assumed that the quenching rate was rapid enough that no defects could anneal out during the quench. However, defects will certainly be able to jump many times on an atomic scale during the quench, maintaining a local defect equilibrium, until all motion ceases at a much lower temperature. If one assumes Newton's law of cooling, it can be shown that K_B depends only on the quenching rate and is independent of the quench temperature, as long as the quenching temperature is greater than an effective temperature below which all motion is frozen. Thus, according to eq. 9, the activation enthalpy should equal the effective formation enthalpy of the Ni-vacancy, independent of binding of the vacancy with the probe. For Schottky equilibrium defects, it equals half the formation enthalpy of the vacancy-pair.

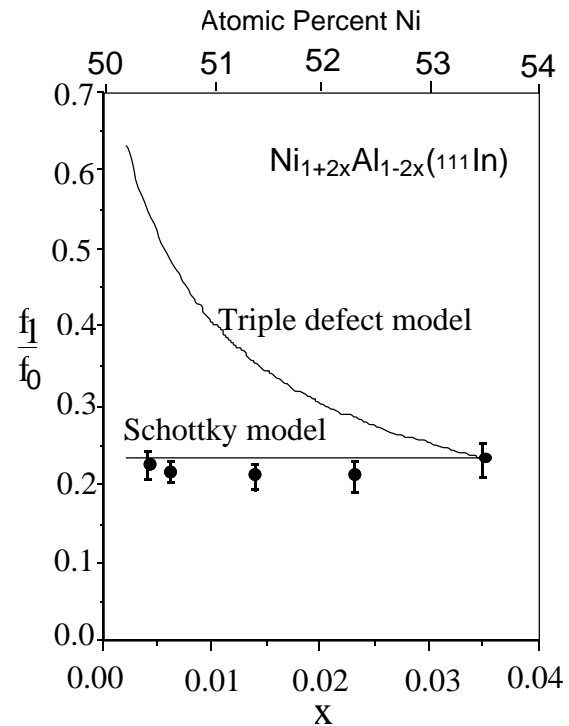


Figure 3: Site fractions of In probes having one Ni-vacancy neighbor as a function of composition measured after quenching from 1050 C. Site fractions, normalized with the defect-free site fraction, are proportional to the vacancy concentration.

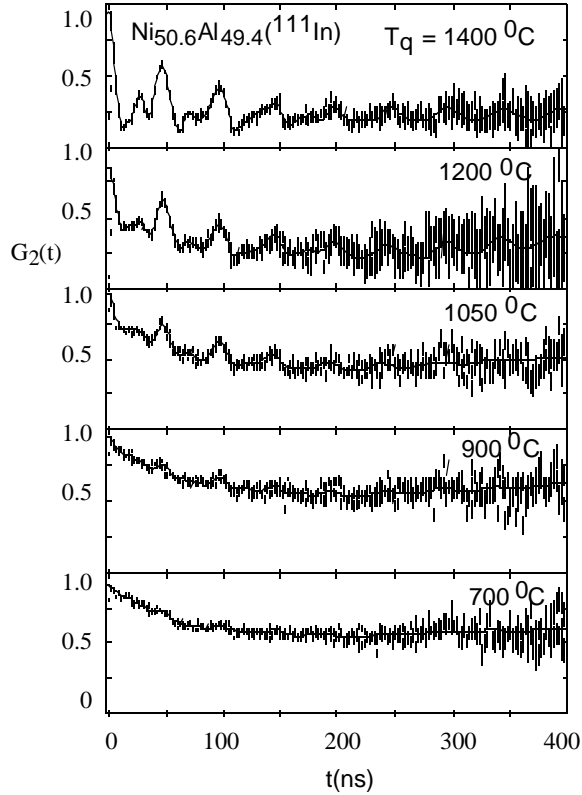


Figure 4: PAC spectra of NiAl after quenching from the indicated temperatures.

3. Low-temperature vacancy mobility

Initial studies of the first stages of annealing-out of quenched-in vacancies led to perplexing results. After quenching a 50.5 at.% Ni sample from 950 C, formation of V_{Ni} -probe complexes was observed to take place at 350 C in 15 min isochronal anneals. This is exhibited in Figure 6, which shows annealing curves for site fractions of the 128 and 141 Mrad/s single-vacancy sites as well as for the sum of both sites. The summed vacancy site-fraction doubles from about 12% to 25% near 350 C, which is attributed to thermal activation and migration of vacancies at that temperature. (9) However, there is no clear-cut evidence of detrapping during annealing at higher temperature that is customarily observed, for example in metals. (15) To understand this odd behavior, a new experiment was undertaken in which samples were prequenched from 950 C to introduce vacancies. Then the samples were equilibrated for 15-minute periods at temperatures at or above 300 C and quenched to room temperature, after which PAC spectra were measured and monovacancy site-fractions determined. It was found that, in the range 350 to 700 C, site-fractions of V_{Ni} could reach equilibrium in 15 minutes and could be altered reversibly by subsequent quenches from higher or lower temperatures. This means that the vacancy concentration remained constant over the entire 350-700 C range, although vacancies were already mobile at 350 C. Site fractions were reversibly found to

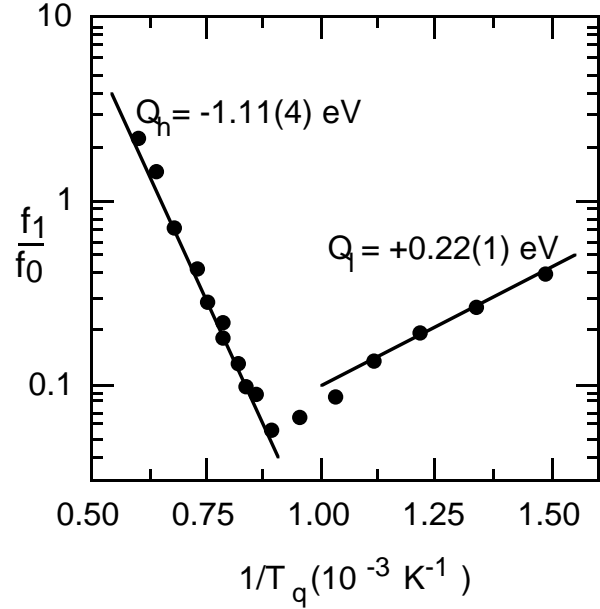


Figure 5: Site fractions of near-neighbor Ni-vacancies versus the inverse quenching temperature. Fractions are normalized by the defect-free fraction. Two equilibrium regimes are observed.

be lower for higher quenching temperature T_q and higher for lower T_q , as expected due to vacancy-probe binding (cf. eq. 9). Finally, irreversible annealing-out of vacancies commenced above about 700 C. In Fig. 5, the low-temperature range shows reversible data obtained in this way. The data were fitted and found to have an activation enthalpy of 0.22(1) eV. According to eqs. 8 and 9, if $[V_{Ni}]$ is constant, the activation enthalpy is the binding enthalpy of the first vacancy.

Such a low-temperature equilibrium regime, in which defects move without annealing out, has not to our knowledge been observed or considered before. It has, however, a natural explanation in terms of different mobilities of the vacancies on the two sublattices: one vacancy species starts to move over atomic distances at 350 C, but is unable to anneal out until the other species becomes mobile at 700 C.

4. Nature of the vacancy species mobile at low-temperature

Which vacancy species becomes mobile at 350 C? The increase in site fraction of V_{Ni} complexes during annealing of quenched NiAl suggests at first sight that V_{Ni} becomes mobile and traps at In impurities at 350 C while V_{Al} becomes mobile at 700 C. However, recent measurements lead us instead to the opposite conclusion: that V_{Al} is mobile at lower temperature.

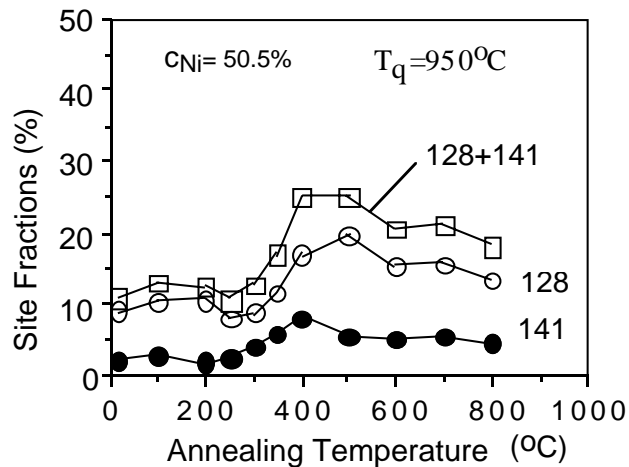


Figure 6. Site fractions for two complexes involving a single Ni-vacancy, and their sum, measured after isochronal annealing of a NiAl sample with quenched-in vacancies. Migration and trapping of vacancies is observed near 350 C.

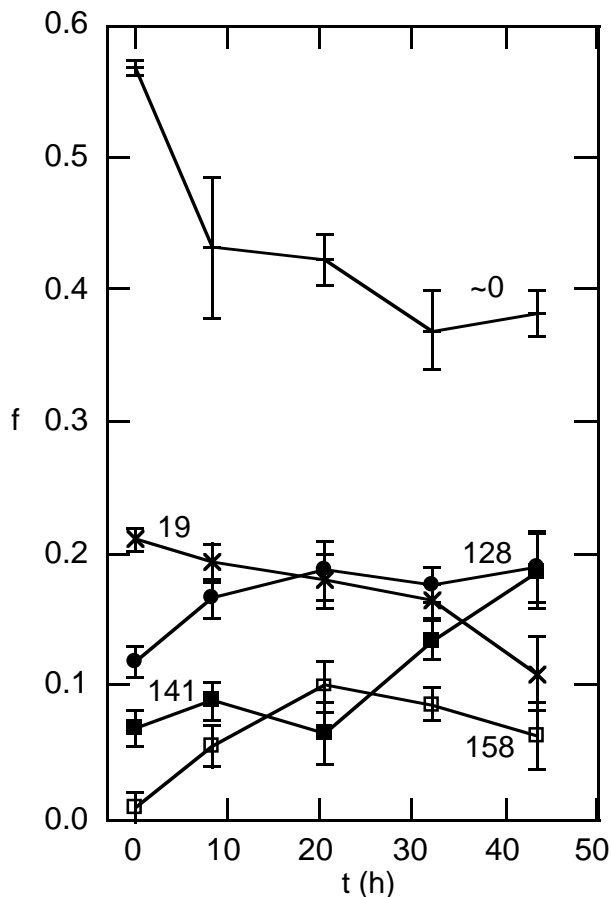


Figure 7: Site fractions of In probes during isothermal annealing at 200 C. Defect identifications are given in Table II.

Recently, we began PAC measurements in equilibrium at elevated temperature instead of on quenched samples. These include measurements undertaken to shed more light on the low-temperature regime as follows. A sample was first prequenched from 950 C. Afterwards, the evolution of site fractions was monitored following annealing for different times at 200 C (see Fig. 7). The equilibration time can be seen from the figure to be of the order of 1 day as opposed to about 15 min. at 350 C, so that atomic motion is indeed very slow even on an atomic length scale. Our findings are as follows:

(1) A new 158 Mrad/s signal is observed during annealing at 200 C that has not previously been detected in very many studies, either after annealing at higher temperature or quenching from high temperature. We conclude that it is not some combination of V_{Ni} and/or Ni_{Al} defects, and that it therefore must involve V_{Al} , the other mobile defect. Most likely, the defect is not an isolated nearby V_{Al} because the observed 158 Mrad/s frequency appears to be too high. In the analog system PdIn we previously detected both V_{In} and V_{Pd} defects and the frequency ratio observed there is only 0.15, much less than 1.23 observed here (cf. Table II). The high frequency therefore suggests that V_{Ni} must be involved. We attribute the signal to complexes involving one V_{Ni} and V_{Al} defect each, as pictured in Fig. 1.j and 1.k. Both configurations have equal efg's in the point-charge approximation. Point charge calculations indicate that the observed frequency can be explained for the two configurations using an effective charge of the V_{Al} equal either to -0.6 or +0.7, which magnitude seems quite reasonable. Therefore, the new signal is attributed to V_{Al} migration and trapping at 350 C.

(2) Site-fractions of both single- V_{Ni} complexes (128 and 141 Mrad/s) are observed to increase during annealing in Fig. 7. While in principle they could form by migration and trapping of V_{Ni} , we found just above that V_{Al} migrates at the lower temperature instead of V_{Ni} and therefore we seek an explanation consistent with a mobile V_{Al} defect. The results can be reconciled by the hypothesis that V_{Al} defects diffuse on the Al lattice until they reach positions in either of Al-shells 2,3 or 5 about the probes. From there, each may react according to eq. 2 with a Ni atom in the first shell, leaving one V_{Ni} in shell 1 and one Ni_{Al} in shell 2,3 or 5. The driving force for the reaction is binding of V_{Ni} to the probes. The reaction and final state are pictured in Figure 8 for V_{Al} reacting after diffusion into shell 3. Depending on the shell from which V_{Al} reacts, the antisite atom may be left in shell 2,3 or 5. If left in shell 2, the final state would be as pictured in Fig. 1.g, with known frequency 141 Mrad/s. If left in shells 3 or 5, then the antisite atom is probably far enough away that the efg's hardly differs from the efg for a lone V_{Ni} (Fig. 1.b) so that the signals are unresolved from the lone V_{Ni} signal at 128 Mrad/s. Therefore, the increases in site fraction of both the 128 and 141 Mrad/s signals in Figs. 6 and 7 can be understood to be caused by migration of V_{Al} with reaction at the probe site.

(3) Conversion of V_{Al} into first-shell V_{Ni} described just above indicates that the 158 Mrad/s complex attributed to the double $V_{Ni} - V_{Al}$ complex may be a less stable state that is only observable during long-time annealing at the very low temperature of 200 C. We suppose that it is unstable at higher temperature, reacting quickly to form one of the double- V_{Ni}

complexes (Fig. 1.c or 1.d). Small increases in double- V_{Ni} site fractions were detected that are not shown in Figs. 6 or 7.

Discussion

1. What is the equilibrium defect in NiAl? Recent theoretical calculations of defect energetics in NiAl, e.g. by local density-functional (16) or embedded atom (5,6) methods find that the triple-defect has lower formation enthalpy than the Schottky vacancy-pair, in contradiction of our findings (Fig. 3 and discussion). Perhaps the best other data for comparison with our measurements are from a high-temperature dilatometric study by Fukuchi and Watanabe (17) who found for samples having 50.9 and 54.5 at.% Ni that, respectively, effective vacancy formation enthalpies were 1.08(6) and 0.96(3) eV, close to our value 1.11(4) eV for 50.6 at.% Ni. They found no increase in the vacancy concentration as the Ni composition decreased toward 50 at.% (indeed a slight decrease was observed), in agreement with our observations in Fig. 3 and in disagreement with the triple-defect model (such as shown in Fig. 2 of ref. 16.) While our identification of a new signal for Al-vacancies near probe atoms supports the Schottky defect model, the attribution is not as direct as we would like. On the experimental side we cannot rule out the possibility of some unknown heterogeneous defect formation mechanism. However, our samples are not atypical of metallurgical samples with regard to grain size, so that if such a mechanism is active here, it should be active in general. On the theoretical side, if, as calculated in ref. 16, the Al-vacancy mole-fraction were never greater than about 10^{-20} , it is difficult to see how a sample could develop an equilibrium concentration of triple-defects in a short time given the presumed second-neighbor diffusion mechanism. To sum up our observations, the Schottky vacancy-pair appears to be the high-temperature equilibrium defect in NiAl.

2. Higher mobility of the aluminum vacancy in NiAl. Our conclusion that the Al-vacancy is more mobile than the Ni-vacancy in NiAl is supported by, and supports, recent embedded-atom-method calculations of energetics of vacancies in NiAl by Mishin and Farkas (5,6) They find that the migration energy of the Al-vacancy should be 0.37 eV lower.

3. Antisite enrichment and diffusion mechanisms. The experiments provide microscopic evidence for migration of both Ni- and Al-vacancies in NiAl and defect interactions with impurity In probes. The reaction $V_{Al} \rightarrow V_{Ni} + Ni_{Al}$ followed by diffusion of the newly-created V_{Ni} away on the Ni sublattice offers a mechanism for enriching local neighborhoods of probes with Ni_{Al} antisite atoms. The fact that observed antisite signals in slightly Ni-rich NiAl have nearly always been much greater than expected for a random distribution of structural defects support this enrichment mechanism. Enrichment might occur because there is binding between antisites and probes or due to an asymmetry between rates of arrival and departure of V_{Ni} and V_{Al} defects.

4. The brittle-to-ductile transition in NiAl. Many intermetallics exhibit a transition from brittle to ductile mechanical behavior at low temperature. In NiAl, this occurs at temperatures of the order of 300 C (see, e.g., 7,18,19). It has been variously attributed to thermal-activation of dislocation

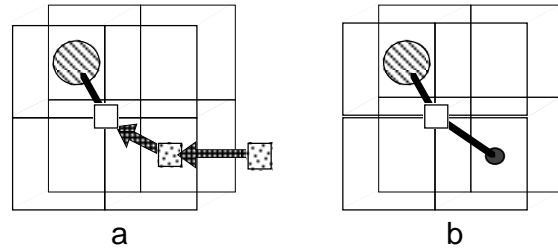


Figure 8: Mechanism by which diffusion of an Al-vacancy can increase the number of Ni-vacancies in the first shell of In probe atoms. (a) Al-vacancy migrates into shell 3 of the In probe and then reacts with a Ni atom (open circle) in shell 1. Vacancy jumps are shown by the arrows. (b) Final defect configuration, with a Ni-vacancy in shell 1 and Ni-antisite atom in shell 3.

motion on new slip systems (18) or to processes mediated by point-defect diffusion (19). Our observation that one of two vacancy species becomes mobile at about 350 C and our identification of the species helps elucidate the nature of the transition. We have demonstrated the presence of a mobile and confined vacancy species, V_{Al} , that can, moreover, transform into the other species, V_{Ni} , at the modest expense of creating an antisite Ni_{Al} defect. As a consequence, the transition to ductile behavior can be explained by the presence of quenched-in (and hard to remove) lattice vacancies that become thermally activated above the transition temperature but which are unable to easily anneal out until the other vacancy species becomes thermally activated. “Free” and mobile vacancies should make possible a broad range of unexpected diffusion processes such as point-defect assisted enhancement of dislocation motion and climb. Brittle-to-ductile transitions in other intermetallics may likewise originate in the different mobilities of point defects.

5. Zirconium solute interactions with vacancies in NiAl. Small amounts of solutes in NiAl cause large changes in mechanical properties. For example, the brittle-to-ductile transition is raised from 300 to 600 C by introducing 0.20 at.% of Zr. (20) Recently we made measurements to determine whether vacancies interact with Zr solutes. (21) In brief, three samples of $Ni_{52}Al_{48}$ having 0, 0.05 and 0.20 at.% Zr were given identical thermal treatments in order to introduce equal, small amounts of excess vacancies, estimated to be about 0.05 at.%. The site fraction of vacancies detected at the ^{111}In probes (at a mole fraction of only about 10^{-8}) was observed to decrease by a factor of three with increasing Zr content. A thermodynamic analysis showed that the trends can be explained by a vacancy-Zr binding enthalpy close to 0.25 eV. In effect, Zr solutes appear to trap and immobilize “free” excess vacancies and make them unavailable to trap at In PAC probes. In the context of our explanation for the brittle-to-ductile transition given just above, presence of Zr solutes (or other solutes that bind with vacancies) depletes free vacancies, thereby making them unavailable to assist in the novel diffusional processes described above, and thus raising the transition temperature.

6. Other B2 intermetallics. PAC measurements have been carried out in this laboratory also on CoAl, FeAl, CoGa and PdIn, with selected results as follows. Annealed stoichiometric samples of CoAl and PdIn exhibit little

inhomogeneous broadening and are therefore very well-ordered in the same way as NiAl. FeAl and CoGa, by contrast, exhibit many signals indicating the presence of intrinsic and/or quenched disorder. Signals analogous to many of those in NiAl were identified in CoAl and PdIn. (22)

CoAl. (ref. 9) Defect behavior was found to be qualitatively similar to NiAl. A high-temperature equilibrium regime was found to extend from 1050 to above 1400 C in which an effective formation enthalpy of 1.55(6) eV for Co-vacancies was obtained from a fit of Co-vacancy site-fractions as in Fig. 5. A low-temperature regime was detected between 550 and 800 C with an activation enthalpy of 0.19(1) eV attributed to vacancy-probe binding.

PdIn. (refs. 14,24,25) The In probe is not an impurity here, so defect concentrations can be determined in a direct way from site-fractions. Supposing that defects are located more-or-less at random, the site fraction of probes having one near-neighbor Pd-vacancy defect, for example, is given by the binomial probability $f_1 = 8[V_{Pd}](1 - [V_{Pd}])^2$. Our measurements follow up on an earlier study by Müller and Hahn. (23) Signals for both V_{Pd} and V_{In} vacancies were detected in quenched PdIn, with thermally activated vacancies detected between 550 and 1250 C. (24) Roughly equal site fractions for the two vacancies were detected, from which it was concluded that the Schottky vacancy-pair is the dominant equilibrium defect. Between 550 and 1000 C, the effective activation enthalpy for formation of Pd-vacancies was determined to be 0.65(9) eV. Above 1000 C, defect concentrations were observed to saturate and not increase further, with $[V_{Pd}] = 1.5$ at.%. A study was also made of defect concentrations in mechanically-milled PdIn. (25) It was found that Pd-vacancy concentrations increase rapidly during the first stages of milling and saturate at a mole fraction of 3.5 at.% after 10 minutes of milling.

Summary

We applied a hyperfine-interaction method with atomic sensitivity, perturbed angular correlation of gamma rays, to study point defects in annealed and quenched NiAl. Because the method differentiates clearly among defects, it can lead to a more model-independent understanding of defect behavior.

Point defects were identified through measurements on annealed, off-stoichiometric samples. Effective formation enthalpies for transition-metal vacancies were determined through analysis of site-fractions of probe atoms in vacancy complexes obtained from quenched samples. The composition dependence of quenched-in vacancies in Ni-rich samples was found to be consistent with the Schottky defect model or, which cannot be excluded, some unidentified heterogeneous formation process.

An explanation was provided for the brittle-to-ductile transition in NiAl (other similar highly-ordered B2 intermetallics) in terms of mobility of quenched-in vacancies: Vacancies are readily quenched into NiAl at levels of the order of 0.1 at.%. Ductility commences at a temperature where one vacancy species, but not the other, can begin to move. This explanation is supported by the finding, briefly described, that Zr solutes trap excess vacancies. Unfortunately, this

explanation does not lead to an obvious solution of the problem of low-temperature brittleness in NiAl. Brittleness can only be made worse by introducing solutes that trap excess vacancies, such as Zr. Solutes that do not trap vacancies should have little effect. PAC experiments are now underway at high temperature to test the assumptions used and conclusions reached here using quenched samples.

Acknowledgments

This work was supported in part by the National Science Foundation under grants DMR 90-14163, 93-13702 and 96-12306 (Metals Program).

References

1. E.g., for NiAl, see A.J. Bradley and A. Taylor, *Proc. Roy. Soc. (London)* A159 (1937) 56.
2. Y. Austin Chang and Joachim P. Neumann, *Prog. Solid St. Chem.* 14 (1983) 221-301.
3. R.J. Wasilewski, *J. Phys. Chem. Solids* 29 (1968) 39-49.
4. Jiawen Fan, PhD dissertation, Washington State University, 1992 (unpublished).
5. Yuri Mishin and Diana Farkas, *Phil. Mag.* A75 (1997) 187-199
6. Yuri Mishin and Diana Farkas, *Phil. Mag.* A75 (1997) 169-185
7. D. B. Miracle, *Acta metall. mater.* 41 (1993) 649-684.
8. C.L. Fu, Y.-Y. Ye, M.H. Yoo and K.M. Ho, *Phys. Rev.* B48 (1993) 6712-6715.
9. Jiawen Fan, PhD dissertation, Washington State University, 1992 (unpublished).
10. B. Lengeler, *Phil. Mag.* 34 (1976) 259.
11. G.S. Collins, S.L. Shropshire and J. Fan, *Hyperfine Interactions* 62 (1990) 1.
12. Jiawen Fan and Gary S. Collins, *Hyperfine Interactions* 60 (1990) 655.
13. Gary S. Collins and Praveen Sinha, *Mat. Res. Soc. Symp. Proc.* 364 (1995) 59.
14. Praveen Sinha, PhD dissertation, Washington State University 1995 (unpublished).
15. F. Pleiter and C. Hohenemser, *Phys. Rev.* B25 (1982) 106.
16. C.L. Fu, Y.-Y. Ye, M.H. Yoo and K.M. Ho, *Phys. Rev.* B48 (1993) 6712.
17. M. Fukuchi and K. Watanabe, *J. Japan Inst. Metals* 43 (1979) 1091 (in Japanese).
18. R.D. Field, D.F. Lahrman and R. Darolia, *Acta metall. mater.* 39 (1991) 2951.
19. R.W. Margevicius and J.D. Cotton, *Acta metall. mater.* 43 (1995) 645.
20. S. V. Raj et al., *Scripta Metallurgica* 23 (1989) 2049.
21. Bin Bai and Gary S. Collins (unpublished).
22. G.S. Collins, P. Sinha and M. Wei, *Hyperfine Interactions* C1 (1996) 580.
23. H.-G. Müller and H. Hahn, *Philos. Mag.* A50 (1984) 71.
24. G.S. Collins and P. Sinha, *Mat. Res. Soc. Symp. Proc.* 364 (1995) 59.
25. G.S. Collins and P. Sinha, *Materials Science Forum* 225-227 (1996) 275.